Electron-Cyclotron Current Drive at the Second Harmonic in the WT-3 Tokamak

H. Tanaka, A. Ando, K. Ogura, S. Ide, M. Iida, K. Oho, S. Ozaki, K. Iwamura, A. Yamazaki,
M. Nakamura, [a] T. Maekawa, Y. Terumichi, and S. Tanaka

Department of Physics, Faculty of Science, Kyoto University, Kyoto 606, Japan
(Received 3 June 1987)

Electron-cyclotron current drive (ECCD) $(\omega = 2\Omega_e)$ is demonstrated for two types of plasma in the WT-3 tokamak. When microwave power P_{EC} is injected into a plasma after Ohmic-heating (OH) power is shut down, the plasma current is sustained and ramped up by the EC wave only. Here $2\Omega_e$ EC-driven current is generated by $2\Omega_e$ EC heating of an energetic electron tail existing in the OH plasma. When P_{EC} is injected into a microwave discharge plasma, $2\Omega_e$ EC-driven plasma current is started up and $2\Omega_e$ ECCD plasma is formed without OH power. The $2\Omega_e$ ECCD efficiency is the same order as that at $\omega = \Omega_e$, but no $3\Omega_e$ EC-driven current is generated, in contrast with theoretical prediction.

In recent years there has been a great interest in noninductive current drive (CD) to realize the steady-state operation of tokamak reactors.[1,2] Experiments have shown successfully that the plasma current is started up,[3-5] ramped up,[6,7] and sustained[8-11] by the lower-hybrid (LH) wave in many tokamaks. Meanwhile, many other noninductive CD methods have been proposed theoretically.[1,2] The electron-cyclotron current drive (ECCD) suggested by Fisch and Boozer[12] is especially important, since it is achieved by asymmetric EC heating along the magnetic field, whose mechanism is quite different from LHCD, and its efficiency including the harmonic waves[13] $(\omega = n\Omega_e, \ n = 1, 2, \text{ and } 3)$ is almost the same as in LHCD. However, there are few ECCD experiments. In the Ohmic-heated (OH) plasma on the TOSCA and CLEO tokamaks, there were different loop voltage drops by $2\Omega_e$ EC waves, propagating in different directions, from which weak EC-driven

currents were estimated.[14] By the injection of an Ω_e EC wave into the WT-2 tokamak, the plasma current $(I_p \simeq 3 \text{ kA})$ was sustained after OH power was shut down.[15,16] In this Letter we report the first experiment in the WT-3 tokamak, in which plasma current $(I_p \simeq 25 \text{ kA})$ is sustained and ramped up by the $2\Omega_e$ EC-driven current without OH power. Here the extraordinary (X) wave is injected from a low-field side and absorbed at $\omega = 2\Omega_e$ without meeting the cyclotron cutoff layer, unlike in the case of Ω_e ECCD.[17] Thus $2\Omega_e$ ECCD is simple in wave propagation and an efficient, localized CD is expected for high-density plasmas, where $\omega_p^2/\omega^2 \leq \frac{1}{2}$.

The experiments were carried out in the WT-3 tokamak,[15] which has an iron core, major and minor radii $R = 65$ and $a = 20$ cm, respectively, the toroidal field $B_t \leq 1.75$ T, and the plasma current $I_p \leq 150$ kA with the aid of feedback control. Microwaves from a gyrotron $(\omega/2\pi = 56 \text{ GHz}, \ P_{EC} \leq 200 \text{ kW}, \ \tau \leq 100 \text{ ms}, \text{ and TE}_{02}$
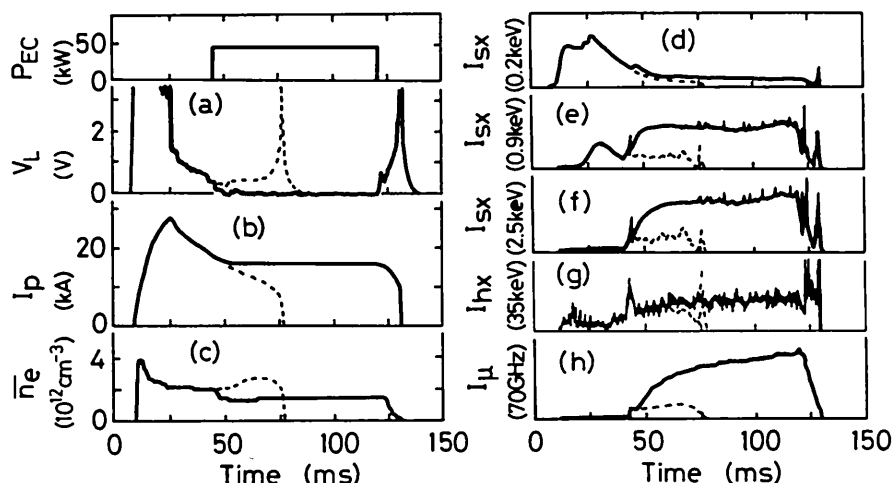

FIG. 1. Temporal evolution of (a) loop voltage V_L, (b) plasma current I_p, (c) line-averaged electron density $\bar{n}_e$ measured by a 4-mm interferometer along the vertical chord, (d) soft x-ray emission I_{sx} (0.2 keV), (e) I_{sx} (0.9 keV), (f) I_{sx} (2.5 keV), (g) hard x-ray emission I_{hx} (35 keV), and (h) electron cyclotron emission I_μ (70 GHz). Full curves are for operation with $2\Omega_e$ EC-heating power $P_{EC} = 48$ kW, $\tau = 75$ ms (parallel injection), and dotted ones without P_{EC}. Initial filling-gas pressure is $p = 8.4 \times 10^{-3}$ Pa in H_2 and additional gas is puffed during P_{EC}. $B_t = 1.09$ T.

mode) were transferred through circular waveguides to a Vlasov antenna with a parabolic reflector placed along the major radius and injected from the low-field side. By rotation of the antenna around the guide axis, a linearly polarized electromagnetic wave, propagating parallel or antiparallel to the toroidal field B_t with an angle of $\pm 60°$, is radiated as the X mode. Further, the electromagnetic wave propagating perpendicular to B_t with inclination of $\pm 60°$ to the horizontal plane is injected as the O (ordinary) mode.

In Figs. 1(a)-1(h) the temporal evolution of plasma parameters with and without P_{EC} is shown. First, a low-density slideaway discharge (dotted curves) with bulk electron density $n_e \simeq 2 \times 10^{12}$ cm^{-3} is produced by OH discharge. When P_{EC} is injected after the primary voltage of the OH transformer is shorted, the plasma parameters change drastically and a constant plasma current I_p continues to flow with loop voltage $V_L = 0$ as long as P_{EC} is applied (full curves). The data show that the plasma is sustained by $2\Omega_e$ EC-driven current only, since no OH current flows for $V_L = 0$. It is noteworthy that in this ECCD plasma (flat-top discharge: 16 kA, 70 ms) strong hard x rays (HXR) I_{hx} ($h\nu > 35$ keV) appear and the soft x-ray (SXR) I_{sx} (0.9 keV), I_{sx} (2.5 keV), and the EC emission I_μ (70 GHz) become more than 10 times as intense as those in OH plasma. This result means that a high-energy electron tail carrying the EC-driven current is generated. On the other hand, the density n_e and SXR I_{sx} (0.2 keV), representing the behavior of bulk electrons, do not change during P_{EC} injection and also the impurity lines I_L (O II-O V) and I_L (C III,C V) do not vary, suggesting that T_e of the bulk electrons does not change and is nearly the same as that in OH plasma. Measurements of Thomson scattering and SXR spectrum analysis show that $T_e = 200 \pm 40$ eV in both OH and ECCD plasmas.

The behavior of the energetic electron tail can be seen from the temporal evolution of the energy spectrum of HXR in Figs. 2(a) and 2(b). The equivalent temperature of the HXR spectrum (curve 1) is $T_{eh} \simeq 40$ keV just before P_{EC} injection. When P_{EC} is applied, T_{eh} in-

creases and attains 90 keV and the maximum photon energy extends to 400 keV at the end of the P_{EC} pulse. At the same time, the photon count ($h\nu > 92$ keV) increases strongly and becomes saturated during P_{EC} injection. After P_{EC} is turned off, I_p and I_{hx} are kept at the same levels within 10 ms, suggesting that the electron tail continues to exist. It is concluded that in this $2\Omega_e$ ECCD plasma the electrons are composed of bulk electrons with $T_{eb} \simeq 200$ eV, $n_e \simeq 2 \times 10^{12}$ cm^{-3}, and an energetic tail with $T_{eh} \simeq 80$ keV, $n_e \simeq 2 \times 10^{10}$ cm^{-3}, carrying $I_p \simeq 25$ kA. In addition, the fact that HXR up to 200 keV is emitted from the initial OH plasma suggests that a weak electron tail is present. For low filling-gas pressure, $p = (0.5-1.2) \times 10^{-2}$ Pa, nonthermal emissions I_μ and I_{hx} appear in the OH plasma; then flat-top discharges are formed and the emissions increase further when P_{EC} is injected. In contrast, for $p > 1.4 \times 10^{-2}$ Pa, these emissions are weak and I_p decreases with time, even if P_{EC} is applied. These results show that the presence of the energetic electron tail in the initial OH plasma is necessary for formation of $2\Omega_e$ ECCD plasma, since asymmetric EC absorption by the tail is strong.[18]

As P_{EC} increases, the $2\Omega_e$ EC-driven current I_p changes from ramp down to flat top, then to ramp up, and $\Delta I_p / \Delta t$ varies from a negative to a positive value [Fig. 3(a)]. Correspondingly, the voltage V_L changes from a positive to a negative value and I_{hx}, I_{sx} (1.7 keV), and I_μ, emitted from tail electrons, increase, while I_{sx} (0.2 keV), emitted from bulk electrons, does not change as P_{EC} increases [Figs. 3(b) and 3(c)]. Further, experiments show that the duration of the flat-top discharge increases, corresponding to the pulse length of P_{EC}. In addition, the $2\Omega_e$ EC-driven current I_p changes from ramp up to flat top, then to ramp down as n_e increases. Correspondingly, V_L changes from a negative to a positive value and the nonthermal emissions, I_{hx}, I_{sx} (1.7 keV), and I_μ, decrease with increasing n_e. These results are very similar to those in LHCD[8] and imply that the current I_p is generated and fully sustained by the $2\Omega_e$ EC wave when P_{EC} is injected into the target plasma having weak tail electrons.
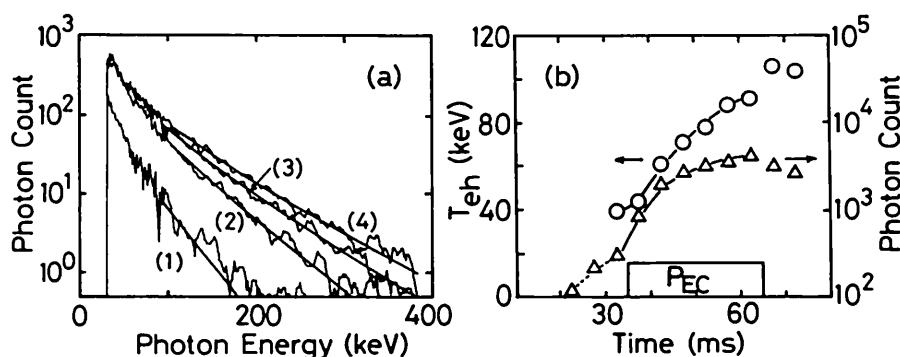

FIG. 2. (a) Energy spectra of hard x rays emitted from the plasma ($P_{EC} = 100$ kW, $\tau = 30$ ms, $I_p \simeq 25$ kA) during time, (1) $t = 30$-25 ms (OH plasma); (2) $t = 40$-45 ms (ECCD plasma); (3) $t = 50$-55 ms; and (4) $t = 60$-65 ms. (b) Temporal evolution of temperature of energetic electron tail, T_{eh} (circles) and photon count with $h\nu > 92$ keV (triangles) as functions of time.
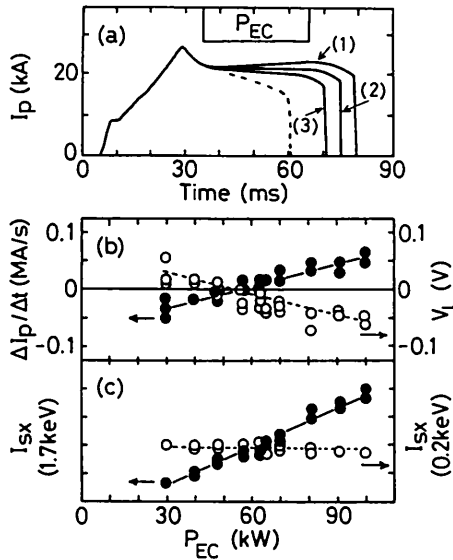
FIG. 3. (a) $2\Omega_e$ EC-driven current ramp-up, flat-top, and ramp-down discharge for various P_{EC}: (1) 100 kW, (2) 57 kW, and (3) 30 kW. Dotted curve is without P_{EC}. (b) Ramp-up rate $\Delta I_p/\Delta t$ (filled circles) and loop voltage V_L (open circles); (c) soft x-ray emissions I_{sx} (1.7 keV) (solid circles) and I_{sx} (0.2 keV) (open circles) as functions of P_{EC}.

The $2\Omega_e$ ECCD is examined by changes in B_t for various wave injection methods in Figs. 4(a)–4(e). As B_t increases, the ratio $\Delta I_p/\Delta t$ during P_{EC} injection approaches zero, becomes positive, and then negative, while it is negative with time constant of $L_p/R_p \simeq 30$ ms in the case of no P_{EC}. Correspondingly, V_L varies from positive to negative, then to positive. Also, nonthermal emissions become intense near the range of $\Delta I_p/\Delta t \geqq 0$, though thermal emission I_{sx} (0.2 keV) does not change with B_t. The flat-top or ramp-up discharge is obtained only when

the field $B_t(0)$ at the plasma center is near $2\Omega_e$ ECR (resonance) $[2\Omega_e(0)/\omega = 1–1.15]$, or the $2\Omega_e$ ECR layer is located at $r(2\Omega_e) = 0–10$ cm. For the perpendicular propagation of the O mode, almost the same curves as in Fig. 4 are obtained. We have examined the temporal evolution of radial profiles of I_{hx} and I_{sx} measured with HXR and SXR detector arrays. When P_{EC} is injected, a broad HXR peak appears and its amplitude increases with time, while the peak position is kept near the center of the plasma ($r \simeq 2.5$ cm). The peak of the SXR profile is slightly outward ($r = 7–8$ cm). These peak positions are not varied by changes in B_t and the wave-injection method. Then it is concluded that the current is generated by $2\Omega_e$ EC heating of the electron tail formed near the plasma center in the initial OH plasma. Such unidirectional tail electrons and their EC heating may eliminate the canceling effect of EC-driven current on the opposite side of the ECR zone. Numerical calculations on $2\Omega_e$ EC absorption along the x-ray trajectory were carried out, including the Doppler and relativistic effects. Single-pass absorption is rather weak ($\simeq 25\%$) and 60% of it is due to the tail electrons. The resonant absorption occurs near $2\Omega_e/\omega = 0.93–1.21$ for $k_\parallel \lesssim 0$, which is consistent with the experimental results in Fig. 4. The fact that the $2\Omega_e$ EC heating effect does not depend strongly on the polarization of the waves may be ascribed to low single-pass absorption and many reflections at the vessel wall.

The $2\Omega_e$ ECCD flat-top discharges of $I_p = 16–27$ kA were obtained in $\bar{n}_e = (1.0–2.3) \times 10^{12}$ cm^{-3} for $P_{EC} = 30–100$ kW. With use of these data, $2\Omega_e$ ECCD efficiency is obtained as

$$\eta_{EC}^{(2)} = \bar{n}_e I_p R/P_{EC} = (2.8–4.4) \times 10^{-2} \, (10^{19} \, \text{A/W m}^2).$$

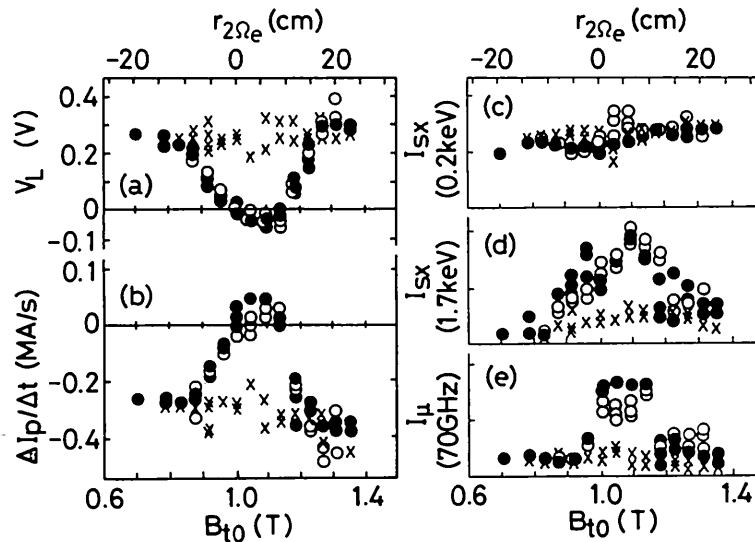This is the same order as $\eta_{EC}^{(1)} \simeq 10^{-2}$ for Ω_e ECCD, and

FIG. 4. (a) Loop voltage V_L, (b) ramp-up rate $\Delta I_p/\Delta t$, (c) SXR I_{sx} (0.2 keV), (d) I_{sx} (1.17 keV), and (e) ECE I_μ (70 GHz) as functions of B_t ($r = 0$) or $2\Omega_e$ EC resonance layer $r(2\Omega_e)$. Filled circles are for parallel injection of P_{EC}, open circles for antiparallel injection, and crosses for OH plasma.

is one order smaller then $\eta_{LH} = (3\text{-}4) \times 10^{-1}$ for LHCD in WT-3.[15] If the quasilinear theory on ECCD given by Cordey et $al.$[13] is applied, with the assumption that the resonant electrons' velocity satisfies $v_{res}/v_{Te} = (T_{eh}/T_{eb})^{1/2} \simeq 20$ and the effective $Z_i = 2$, the ECCD efficiency is calculated as $\eta_{EC}^{(n)} = 1.0\text{-}1.2$ for $n = 1$, 2, and 3. This value may be reduced below $\frac{1}{2}$ if the trapped electrons' effect is considered. However, the experimental values of $\eta_{EC}^{(n)}$ for $n = 1$ and 2 are one order smaller. It is noted that $3\Omega_e$ ECCD is not observed in Fig. 4, where $3\Omega_e(0)/\omega = 1$ at $B_t(0) = 0.67$ T, in contrast with the above theoretical prediction.[13] On the other hand, the $3\Omega_e$ EC damping rate is T_e/mc^2 ($\ll 1$) times smaller than those at $\omega = \Omega_e$ and $2\Omega_e$, suggesting that $3\Omega_e$ ECCD is not formed. Further, the experiments show that the ratio is $\eta_{EC}/\eta_{LH} \simeq 0.1$, while it is $\frac{3}{4}$ by the theory.[12] The reason for these discrepancies may be as follows: The theory treats high-T_e thermal plasmas, while the experiments are carried out for low-T_e plasmas with the energetic electron tail where bulk electrons absorb ECW and produce no EC-driven current. So it cannot apply directly to the theoretical calculation.

The $2\Omega_e$ EC-driven current is also generated in a microwave discharge at ECR with a small gyrotron (40 GHz, 10 kW, 5 ms), where the primary coil of an OH transformer is shorted. When P_{EC} (56 GHz, 100 kW, 30 ms) is injected into this ECR plasma, the plasma current is started up with the rate of $\Delta I_p/\Delta t \simeq 70$ kA/s and $V_L \simeq -0.2$ V, and attains $I_p^{(m)} = 2$ kA at the end of P_{EC}. The density of bulk electrons is low ($n_e \simeq 0.7 \times 10^{12}$ cm^{-3}), and nonthermal emissions appear at the late stage and increase strongly with I_p, suggesting that an energetic electron tail is produced. These $2\Omega_e$ EC-driven currents are generated in the field range of $B_t(0) = 0.92\text{-}1.22$ T $[2\Omega_e(0)/\omega = 0.92\text{-}1.22]$ and the maximum current is obtained at $B_t(0) = 1.09$ T $[2\Omega_e(0)/\omega \simeq 1.09]$. The experimental curves, $I_p^{(m)}$ vs $B_t(0)$, are almost the same among wave injection methods and $I_p^{(m)}$ decreases in the order of $k_\parallel > 0$, $k_\parallel < 0$, and $k_\parallel = 0$. The current $I_p^{(m)}$ increases with P_{EC}, though I_p does not start up below $P_{EC} = 40$ kW. The $2\Omega_e$ ECCD plasma is formed at $p = (0.3\text{-}1.5) \times 10^{-2}$ Pa, and $I_p^{(m)}$ and the nonthermal emissions I_{sx} (1.7 keV) and I_μ decrease, while the thermal emission I_{sx} (0.2 keV) increases as p increases. In these ECR plasmas, an asymmetric velocity distribution of electrons along B_t is formed when the vertical drift of electrons is canceled by the vertical field B_v. Here, the direction of I_p is determined by B_v and independent of k of the EC waves as shown by the experiments. Thus it is concluded that the asymmetric tail electrons are enhanced by $2\Omega_e$ EC heating of the tail electrons whose velocity distribution is asymmetric since there is a difference in the confinement

time among electrons moving along B_t.

In conclusion, the $2\Omega_e$ EC-driven current is generated in two types of plasma. First, such current is generated by $2\Omega_e$ EC heating of the energetic electron tail and the plasma current is sustained or ramped up after OH power is shut down. Second, $2\Omega_e$ EC-current-driven plasma is formed by $2\Omega_e$ EC heating of the energetic electron tail in the ECR plasma. In the experiments, the $3\Omega_e$ EC-driven current is not generated, in contrast with the theoretical prediction.[13] The $2\Omega_e$ ECCD method is useful in tokamaks, since EC wave propagation and damping processes are simple and high power sources such as gyrotrons and free-electron lasers are developing. The ECCD efficiency is low in the present experiments; however, it is suggested by theory[18] and experiment[16] that the combined effect of EC and Landau damping is high, though detailed experiments are necessary.

(a)Permanent address: Osaka Institute of Technology, Osaka 535, Japan.

[1]N. J. Fisch, Rev. Mod. Phys. **59**, 175 (1987).

[2]$Non\text{-}Inductive$ $Current$ $Drive$ in $Tokamaks$, edited by D. F. H. Start (Culham Laboratory, Abingdon, United Kingdom, 1983), Vols. 1 and 2.

[3]S. Kubo et $al.$, Phys. Rev. Lett. **50**, 1994 (1983), and J. Phys. Soc. Jpn. **53**, 1047 (1984).

[4]K. Toi et $al.$, Phys. Rev. Lett. **52**, 2144 (1984).

[5]F. C. Jobes et $al.$, Phys. Rev. Lett. **52**, 1005 (1984).

[6]F. C. Jobes et $al.$, Phys. Rev. Lett. **55**, 1295 (1985).

[7]N. J. Fisch and C. F. F. Karney, Phys. Rev. Lett. **54**, 897 (1985).

[8]M. Nakamura et $al.$, Phys. Rev. Lett. **47**, 1902 (1981), and J. Phys. Soc. Jpn. **51**, 3696 (1982), and **53**, 3399 (1984).

[9]S. Bernabei et $al.$, Phys. Rev. Lett. **49**, 1255 (1982).

[10]M. Porkolab et $al.$, Phys. Rev. Lett. **53**, 450 (1984).

[11]K. McCormick et $al.$, Phys. Rev. Lett. **58**, 491 (1987).

[12]N. J. Fisch and A. H. Boozer, Phys. Rev. Lett. **45**, 720 (1980).

[13]J. G. Cordey et $al.$, Plasma Phys. **24**, 73 (1982).

[14]D. C. Robinson et $al.$, in $Proceedings$ of the $Eleventh$ $International$ $Conference$ on $Plasma$ $Physics$ and $Controlled$ $Nuclear$ $Fusion$ $Research,$ $Kyoto,$ $Japan,$ 1986 (IAEA, Vienna, 1986) Paper No. IAEA-CN-47/F-III-2.

[15]S. Tanaka et $al.$, in Ref. 14, Paper No. F-II-6.

[16]A. Ando et $al.$, Phys. Rev. Lett. **56**, 2180 (1986), and Nucl. Fusion **26**, 107 (1986), and J. Phys. Soc. Jpn. **55**, 4259 (1986).

[17]R. O. Dendy et $al.$, Nucl. Fusion **27**, 377 (1987).

[18]I. Fidone et $al.$, Phys. Fluids **27**, 661, 2468 (1984), and **29**, 803 (1986).